Method to estimate the ground loads for missing periods in a monitored GSHP

Anjan Rao Puttige[1], Staffan Andersson[1], Ronny Östin[1], Thomas Olofsson[1]

[1] Umeå University, Umeå, Sweden

anjan.puttige@umu.se

Keywords: ground source heat pump, borehole heat exchanger, monitored, missing loads.

ABSTRACT

Monitoring a ground source heat pump can provide important insights into its working, but to study the behaviour of the borehole heat exchanger (BHE) we require monitored data for the whole period of operation. In practice, the monitored data often has periods of missing data. We propose a method to estimate the load during the periods of missing data based on the fluid temperature after that period. The method determined the missing load with negligible error, for the case of a BHE that behaves exactly like the model describing it. A sensitivity analysis showed that the estimated load is highly sensitive to errors in measured load and fluid temperature. The method was applied to a real monitored BHE, the magnitude of estimated loads were unreasonably high, but the overall deviation between the measured and simulated values of fluid temperature decreased. Therefore, the high magnitude of missing load compensates for the lack of agreement between the model and the measured data.

1. INTRODUCTION

Ground source heat pumps (GSHP) use the ground as a source/sink for a heat pump instead of the ambient air. GSHP can offer higher efficiency compared to conventional heat pump because the temperature underground has smaller fluctuations (Yang et al. 2010). Although the concept of a GSHP has been around for more than a century, the technology became widely used after the oil crisis in 1973 (Sanner 2017). Since then, design and operation of GSHP has been an active research area. Data obtained from monitoring the operation of real GSHP play an important role in this research. There are several examples of monitored data of GSHP being used to evaluate design procedures, diagnose poor performance and explore opportunities for improvements in performance of a GSHP system.

Michopoulos et al. (Michopoulos et al. 2007, Michopoulos et al. 2013) used the monitored data to demonstrate the advantages of a GSHP compared to conventional heating and cooling system in northern Greece. A more common application of monitored data is to validate models of GSHP, especially the borehole heat exchanger (BHE). Ruiz-Calvo et al (Ruiz-Calvo and Montagud 2014, Ruiz-Calvo et al. 2016) presented 11 years of monitored as a reference to validate models. Monzo et al. (2018) and De Rosa et al (2015) used this data to validate their model of BHE. Naiker and Rees (2011) also presented the motoring data of a BHE used in a large building to be used for validating models. Cullin et al (2015) used monitored data from 4 BHE to show that simulation based design tool is more accurate than the design equation given in ASHRAE handbook for determining required length of the borehole. Hellström et al (1997) used monitored data to validate their design software EED. The validated models can be used for design of new BHE or modify the operation of exsisting GSHP. Kim et al (2010) used their monitored data to validate their numerical model, and then used the verified model to evaluate the design and study the effect of change in operation scheme of the system. The monitored data can also be used to calibrate the model as demonstrated by Tordrup et al (2017) and Fernandez et al (2017). Esen et al. used monitored data to develop data driven models based on artificial neural network (ANN) (Esen et al. 2008), adaptive neuro-fuzzy inference systems (ANFIS) (Esen et al. 2008) and support vector machine (Esen et al. 2008). McDaniel et al (2018) used the monitored data to show the importance of effects of groundwater flow and long term effects of heat storage in a large scale BHE, by measuring the temperature along the length of the borehole using optical fibers.

These examples demonstrate the usefulness of monitored data in development of GSHP, but a common problem reported by many of these examples (Hellström et al. 1997, Kim et al. 2010, Naiker and Rees 2011, Ruiz-Calvo and Montagud 2014, Ruiz-Calvo, et al. 2016) are missing data. The missing data could be caused by a shutdown in the monitoring system for maintenance or due to faults, in some cases the monitoring system is installed after operation of the GSHP begins. Availability of the whole data set is especially important for GSHP due to the high thermal capacity of the ground, which results in loads during the missing periods affecting the performance of the GSHP for a long time after the period. Hence, in the previous studies the loads during the missing periods are estimated by using the ambient temperature (Monzo et al. 2018) or by using the load of another year (Hellström et al. 1997), whereas Kim et al (2010) excluded a part of the GSHP due to the missing data.

In this paper we propose a method to estimate the loads during the missing period by studying the effect of the load on the measured temperature of the working fluid

after the period of missing data. The proposed method is outlined in chapter 2. A monitored GSHP that has been operational for about 3 years is used to develop and demonstrate this method, chapter 3 has a description of the GSHP. Chapter 4 describes the model chosen to represent the BHE. The method is developed for an ideal case in chapter 5 and it is applied to the real case in chapter 6.

2. PROPOSED METHOD

We present a method to use the thermal inertia of the ground to estimate the load in the periods missing data. The loads in the missing periods influences the temperature of the fluid in the borehole heat exchanger after the period. Therefore, the measured fluid temperature is used to predict the load during the period without data.

The heat load during the period of missing data is assumed to be a constant. The unknown heat load along with known heat loads from the period when measured data is available are used as input to a model that predicts the fluid temperature in the borehole heat exchanger. The fluid temperature can be expressed as a function the unknown and known loads

$$T^n_{fsim} = f(Q_e, Q_{m1}, Q_{m2}, \dots Q_{mn}) \qquad [1]$$

Where T^n_{fsim} is the simulated fluid temperature at the time step n, Q_e is the average load during the period without measured data, Q_{mi} are average measured load for the time step i. The function (f) is a representation of the model. There are a number of analytical or numerical models available in literature (Yang et al. 2010, Li and Lai 2015, Atam and Helsen 2016), each with its advantages and disadvantages.

The value of the unknown heat load is determined such that the difference between the measured and simulated values of the fluid temperature is minimised. The objective function of the minimisation is expressed in equation 2

$$R = \sum(T^i_{fsim}(Q_e, ..) - T^i_{fm})^2 \qquad [2]$$

Where T^i_{fm} is the average measured fluid temperature for time step i.

Determining the range of i requires some consideration. Since we considered the load in the unknown period to be a constant, we cannot have a high time resolution immediately after the period of unknown loads. The variation in the loads can only be ignored after certain period of time. The idea that only the average load for a period is significant after certain period of time has been successfully used by load aggregation methods (Yavuzturk and Spitler 1999, Bernier et al. 2004, Claesson and Javed 2012) which use this trait to reduce the computational time to calculate borehole wall/ fluid temperatures. In this study the time frames recommended by Claesson and Javed (2012) are used to determine the time steps immediately after the missing period. The normal time step for the simulation is chosen as 1 day, therefore the time steps used are 1, 2,,..2^n, number of days of missing data, n is chosen such that 2^n is less than number of days in missing period. The aggregated steps are used until the fluid temperature can be determined with a time resolution of 1 day. The first day with a time resolution of 1 day is chosen as the starting value of i in the objective function of the minimisation function.

The upper limit of i must be large enough so that the random errors in the measured values of Q_{mi} and T^n_{fm} are negated, but the influence of the missing load decreases over time and fluid temperatures that are not significantly influenced by the missing load must not be used to estimate it. Hence we must determine a period of time when the missing load has a significant influence on the fluid temperature.

3. GSHP DESCRIPTION

The method described in the previous chapter is developed and demonstrated using a GSHP that has been monitored since February 2016. The GSHP was installed in a hospital building in Umeå to reduce the dependency on the district heating and cooling. The GSHP was designed to produce 7 GWh of heat and 5 GWh cooling annually. The GSHP covers 95% of the cooling load of the building and 20% of the heating load the rest of the load is covered by an air source heat pump and district heating and cooling. A schematic of the system is shown in figure 1. Heat pump 1 and 2 provide space heating while heat pump 3 provides domestic hot water and excess heat for space heating when required. The GSHP can be used in both free cooling mode and active cooling mode depending on the cooling needs of the building. In summer, the BHE is also used for storing excess heat from the condenser.

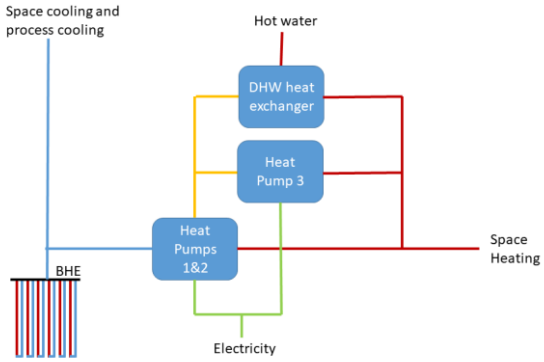

Figure 1: Schematic of the GSHP system

The BHE consist of 125 boreholes divided into two groups of 62 and 63 boreholes. The two groups have separate hydraulic loops but due to their close proximity they are thermally connected. The loads of borehole groups are different especially in summers when excess heat from the condenser is stored in borehole group A while borehole group B is used for heating. The boreholes in borehole field A are 200 m deep while the boreholes in borehole group B are 250m. The boreholes are similar in all other aspects. Each borehole has a diameter of 140 mm and consists of a single U-tube. The distance between the boreholes is

7m and the ground water level is 10m. The thermal properties of the ground were estimated by performing a thermal response test on a 250m deep borehole. The volumetric heat capacity of the ground was taken from the available geological data. Table 1 lists the properties of the ground and the geometry of the BHE.

Table 1: Geometric and thermal properties of the BHE

Property	Value
Borehole radius (r_b)	0.070 m
Borehole depth (H+D)	200 m/250 m
Ground water level (D)	10 m
Thermal conductivity of the ground (k)	3.4 $W(mK)^{-1}$
Volumetric heat capacity of the ground (ρCp)	2.3×10^6 $JK^{-1}m^{-3}$
Borehole resistance (R_b)	0.08 mKW^{-1} (0.11 mKW^{-1} for extraction)
Undisturbed ground temperature (T_{ug})	5.9^0C

The operation of the GSHP has been monitored from the start of its operation on 16th February 2016. The inlet and outlet temperatures of each borehole group was monitored using temperature sensors for each borehole group. Flow and energy meter were installed for each borehole group on 15th March 2017. Until the flow meters were installed, the flow was estimated from the power of the circulation pumps. Flow rate and percentage of pump power were found to have a strong correlation. Figure 2 shows the relation between hourly flow rates and relative pump power w.r.t. its maximum power for the period from 15th March 2017 to 31st December 2018. The relation is linear for 96.6% of the points, but for the rest of the points the flow rate is approximately 1/10th of the predicted by the linear relation. It was observed that these odd points occur on specific periods, 2017/05/18-2017/05/19 and 2017/06/19-2017/07/03. The temperature values for these period are within normal operating range, which indicates that the reason for such behavior was most likely due to a fault in the monitoring system. Hence, the odd flow measurements were discarded and the relation between the pump power percentage and flow rate was established using rest of the flow measurements. The correlation coefficient of the linear relation is 0.98, therefore we consider the flow rate calculated during these periods to be a good approximation. The linear relation was used to calculate the flow rate for the period before the flow meter was installed and during the odd measurements of flow meter.

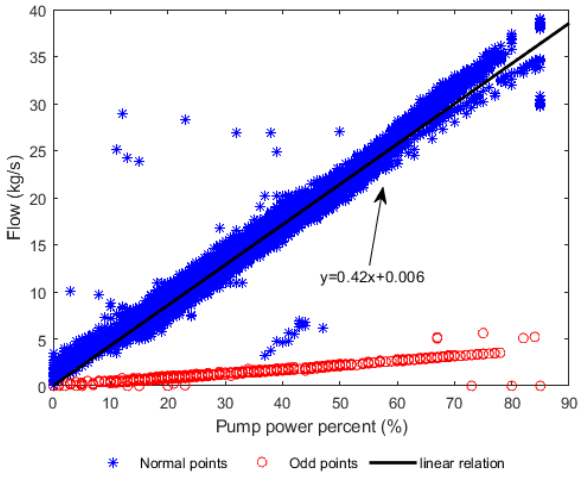

Figure 2: Relation between flow and relative pump power

There are 87 days between 16th February 2016 and 31st December 2018, when no measured data is available. These gaps in data are due to shut down for maintenance or due to other errors in the measurement system. Figure 3 shows the measured ground loads and highlights the gaps in the data using boxes. The method described in chapter 2 will be used to estimate the loads for these gaps in the data. Note that the negative loads corresponds to injection and positive loads corresponds to extraction.

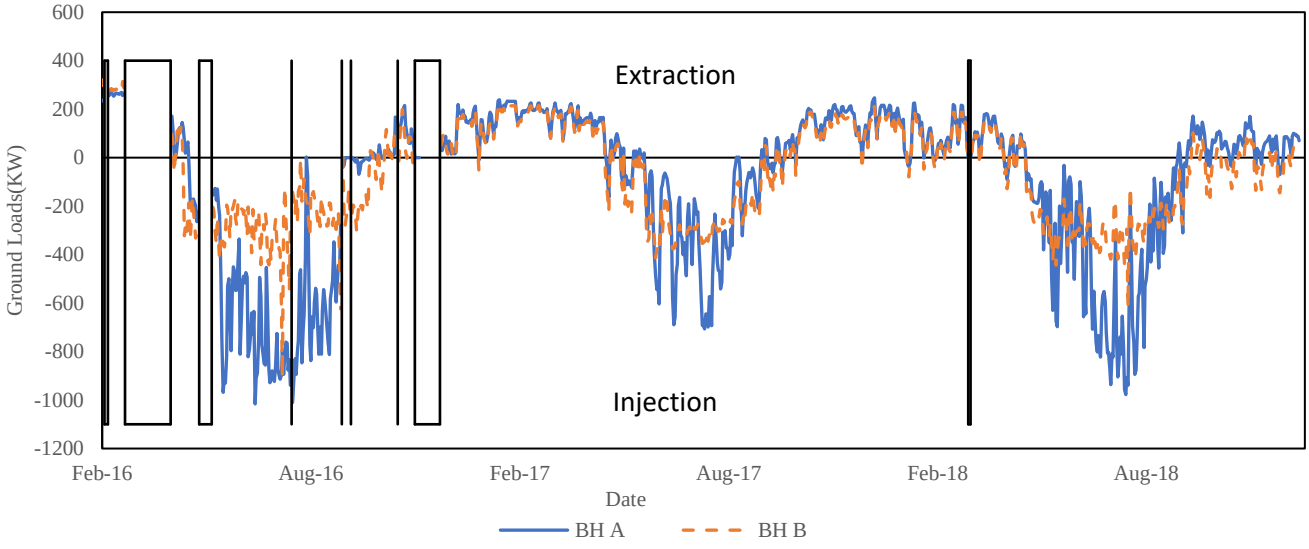

Figure 3: Measured loads with missing data highlighted using boxes

4. MODEL DESCRIPTION

We require a model to determine the simulated values of fluid temperature. In this case we chose the model presented by Lamarche (Lamarche 2017). An analytical model was chosen because the BH field is large and the model needs to run multiple times to find the minima, hence the computational time of a numerical model would be too long in this case. Borehole group A and B have separate inlets and outlets but they have to be considered as a single BH field. The chosen model is one of the few analytical models that allow multiple inlet conditions for a BH field. The model has two key features. First it uses 'non-history' scheme proposed in (Lamarche 2009) to calculate the temperature at the borehole wall. This approach divides the change in borehole temperature into two parts one corresponding to the effect of load in the current step and another that corresponds to the effect of previous loads. Second, it considers the responses of individual boreholes on each other separately which allows us to have different heat fluxes for each borehole. The model can be summarised by the following equations, a detailed explanation of the model and how to implement it can be found in (Lamarche 2017). The borehole wall temperature for borehole i ($T_{b,i}$) is calculated using the inlet fluid temperature ($T_{fin,i}$)

$$T_{b,i} = S_{p,i} + \sum_{j=i}^{nb} S_{q,ij} X_j \left(T_{fin,j} - T_{b,j}\right) \quad [3]$$

$S_{p,i}$ corresponds to the effect of the previous loads on borehole i, while the second term corresponds to the effect of the current load, . $S_{p,i}$ are updated at every time step using equation 5.

$$s_{p,i} = \frac{1}{k} \sum_{l=1}^{Nz} e^{-z_l^2 \Delta \bar{t}} F_i^n(z_l) \Delta z_l \quad [4]$$

$$F_i(\bar{t} + \Delta \bar{t}, z_l) = e^{-z_l^2 \Delta \bar{t}} F_i(\bar{t}, z_l) + \sum_{j=1}^{nb} q_j'(\bar{t}) \left(1 - e^{z_l^2 \Delta \bar{t}}\right) u_{ij}(z) \quad [5]$$

$$F_i(0) = 0 \quad [6]$$

Where u_{ij} is defined by equation 5. In equation 5, g_{ij} is the effect of a single borehole on a borehole at a distance r_{ij}. This is calculated by finding the average non-dimensional temperature at the borehole wall using the finite line source approach presented in (Zeng et al. 2002)

$$u_{ij}(z) = -2zL^{-1}\left(\frac{g_{ij}}{2\pi}\right) \quad [7]$$

$S_{q,ij}$ is the coefficient that related to temperature effect of borehole i due to the heat flow in borehole j. X_i is a coefficient that used to convert the heat load q_i to the temperature difference ($T_{fin,i}$-$T_{b,i}$).

$$S_{q,ij} = \frac{1}{k} \sum_{l=1}^{Nz} \left(1 - e^{-z_l^2 \Delta \bar{t}}\right) u_{ij}(z_l) \Delta z_l \quad [8]$$

$$X_i = \frac{\dot{m}_i C_p}{H_i} (1 - \theta_i'') \quad [9]$$

We used the linear approximation for θ¨, given by equation 10

$$\theta_i'' = \frac{1 - Y_i}{1 + Y_i} \quad [10]$$

$$Y_i = \frac{H_i}{2\dot{m}_i C_p R_b} \quad [11]$$

In the above equations both T_{fin} and T_b are unknown hence we have relate T_{fin} to the loads using the following equations

$$T_{fin,i}|_{i=1,2\ldots62} = T_{fin,A},\ T_{fin,i}|_{i=63,64\ldots125} = T_{fin,B} \quad [12]$$

$$Q_A = \sum_{i=1}^{62} q_i' H_i = \sum_{i=1}^{62} (T_{fin,A} - T_{b,i}) X_i H_i$$
$$,\ Q_B = \sum_{i=63}^{125} q_i' H_i = \sum_{i=63}^{125} (T_{fin,B} - T_{b,i}) X_i H_i \quad [13]$$

The outlet temperatures ($T_{fout,i}$) can be calculated using T_{fin} and T_b using the following equation

$$T_{fout,i} = \theta''_i T_{fin,i} + T_{b,i}(1 - \theta''_i) \quad [14]$$

5. SYNTHETIC RUN

Measured load from a year of uninterrupted data is used to calculate the ideal fluid temperatures using the model. This set of data is referred to as 'synthetic data'. The first 32 days of this data set is then considered to be the missing period and the average load for the missing period is estimated by using the load estimation method. Synthetic data allows us to evaluate the load estimation method disregarding any measurement and model errors and also determine the accuracy of the method.

5.1 Ideal case test

To determine the missing load, first a suitable aggregation scheme is chosen. The aggregation scheme must determine the fluid temperature with the same accuracy as complete 1 day simulation. The missing load is then determined such that the objective function defined in equation 2 is minimized.

The number of missing days in this case is 32 days hence we choose 32 day time step as the lowest time resolution in the aggregation scheme (Claesson and Javed 2012) and one day as the highest time resolution. We used 6 steps of different time resolutions, each half of the previous one, i.e., 32, 16, 8, 4, 2 and 1 day. This means that the first day with 1 day time resolution is the 63rd day of operation (32+16+8+4+2+1).

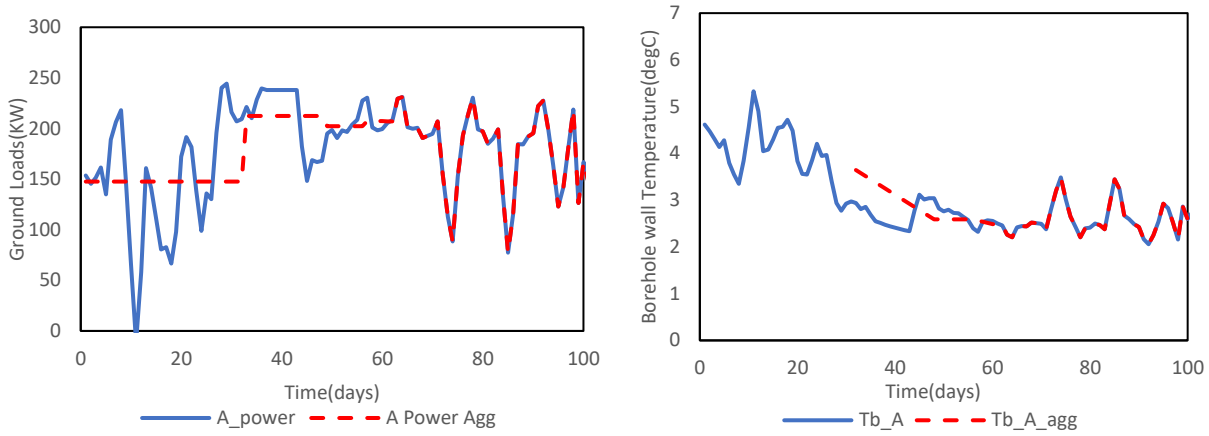

(a) (b)

Figure 2: Comparison of aggregated and non-aggregated load and temperature

Figure 4a shows the daily loads for borehole group A and the aggregated loads calculated by averaging the daily loads for the aggregated periods and Figure 4b shows borehole wall temperature obtained from the two loads, the temperatures have a good agreement after the aggregated periods. This shows that the aggregation scheme does not lead to any loss in accuracy.

The average load for the missing period is now considered to be unknown Q_e. Q_e is determined by using the procedure described in chapter 2. The first day used in the minimization objective function is 63, the first day with 1 day time step, since there is no measurement or model error the number of days used for minimization is not important in this case, 5 days of fluid temperature were used for minimization. The average loads for the missing period was estimated to be 147.599 KW and 130.005 KW for the two fluid loops, the synthetic measured load for the same period was 147.597 KW and 130.022 KW respectively. The negligible difference between the estimated and synthetic measured loads can be attributed to numerical error of the optimization algorithm. The agreement between the estimated and synthetic measured data proves that this method of load estimation works in an ideal case

5.2 Number of days after missing data

To determine the number of days used for minimization we must determine the period of time where the effect of the unknown load has a significant effect on the fluid temperature. In order to quantify the effect of the effect of the unknown load without using the load we use g-function and defined g-effect in equation 15

$$g_{effect}(t) = (g(t) - g(t - t_{uk}))/g(t) \quad [15]$$

g(t) is the g-function of the borehole field at time t and t_{uk} is the time period of missing load, 32 days in this case. g-effect is the ratio of effect of borehole wall temperature of a load from time 0 to t_{uk} compared to a load from time 0 to t.

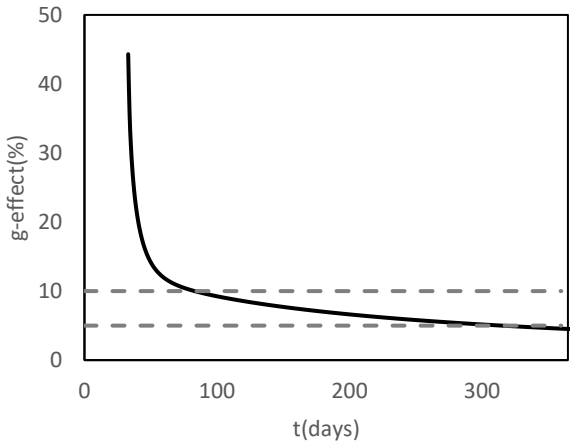

Figure 3: Variation of g-effect with time

Figure 5 shows the g-effect for the borehole field with t_{uk} of 32 days. In this study two threshold values will be studied, 5% and 10%. 10% corresponds to 83 days or 21 days of 1 day time steps, 5% corresponds to 315 days or 253 days of 1 day time steps.

The g-effect was used to modify the objective function for minimisation, difference between simulated and measured fluid temperatures was weighted by the g-effect. Hence the weights are proportional to the effect the missing loads has on the fluid temperature.

$$R' = \sum g^i_{effect}(T^i_{fsim}(Q_{uk},..) - T^i_{fm})^2 \quad [16]$$

5.3 Sensitivity of estimated load

The estimated load depends on measured loads and the measured fluid temperatures. Sensitivity analysis was performed to understand how error in these quantities effects the estimated load. Sensitivity analysis was performed for both 10% g-effect cut off and 5% g-effect cut off.

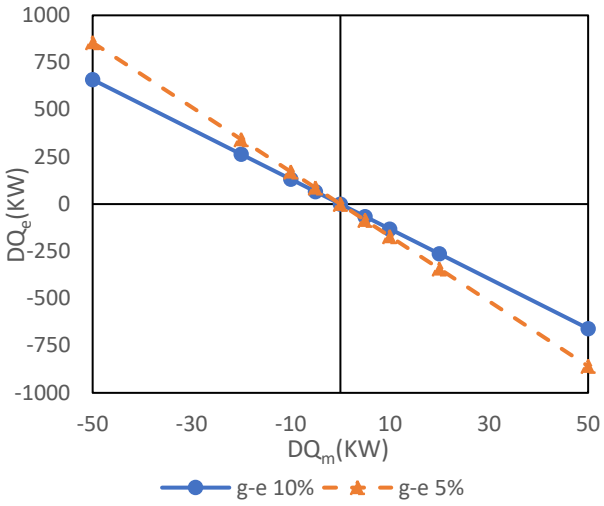

Figure 4: Sensitivity of the estimated load to the measured load

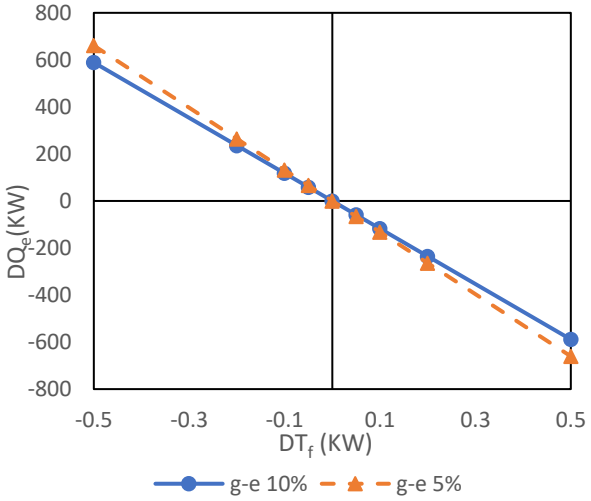

Figure 5: Sensitivity of the estimated load to the measured fluid temperature

Figure 6 and 7 shows how the error in measured loads (DQ_m) and error in fluid temperature (DT_f) effects the estimated load (DQ_e). 'g-e 10%' represents the case where g-effect of 10% is used as cut-off and 'g-e 5%' represents the case of 5% g-effect cut-off. DQ_e has linear relation to both DQ_m and DT_f and the slope represents the sensitivity of Q_e to the two inputs, the slope of the lines is shown in table 2. An increase in Q_m results in underestimation of Q_e so that the error in simulated values of T_f is reduced. DQ_e must compensate for the error for error in Q_m, due to longer time duration of Q_m and closer proximity to T_f the sensitivity DQ_e/DQ_k is high. An increase in the measured T_f must be compensated by increasing the injected heat, since heat injected is represented by –Q, DQ_e is negative. The accuracy of Q_e is highly sensitive to the error in Q_m and T_f.

Table 2: Sensitivity of the estimated load

Parameter / g-effect cut off	Sensitivity	
	Q_k (KW/KW)	T_f (KW/K)
g-e 10%	-13	-1177
g-e 5%	-17	-1321

The daily average measured values of Q_m and T_f are determined using measurements of time resolution of 5 minutes, hence random measurement error is negligible. However the main source of error in Q_e is likely to originate from the shortcomings of the theoretical models ability to represent that behavior of the actual BHE, for instance inhomogeneity, ground water flow etc. But Q_e is expected to compensate for the inaccuracy of the model to some extent, consequently leading to a better agreement between the simulated and the measured values of T_f.

6. REAL CASE

The method developed to estimate the loads for the missing period was applied to the measured data described in chapter 3. The details of missing periods is listed in table 3 with the number of days of missing data (N_miss), number of days of continuous data after the missing period (N_after), number of days after the missing period when a time resolution of 1 day can be used (N_day), number of days after which the g-effect of the missing period is 10% (N_10%) and number of days after which the g-effect of the missing period is 5% (N_5%). To apply the method, the following condition must be satisfied

$$N\_day \leq N\_10\% \leq N\_after \quad [17]$$

$$N\_day \leq N\_5\% \leq N\_after \quad [18]$$

If N_10% is less than N_day, g-effect of the first day with 1-day time resolution will be less than 10% hence the method cannot be applied. If N_10% is greater than N_after, we will not have enough continuous data points after the missing period to apply the method. For the missing period 2, highlighted in red, N_after is less than both N_5% and N_10%, therefore we cannot apply the method for this period. The correlation between the ambient temperature and load was used to determine load in this period. In the periods 3 and 8, highlighted in yellow, N_10% is lower than N_day which means that the g-effect on the first day with 1 day resolution is less than 10%. In this case, Q_e was determined using only the first day of 1 day time resolution.

Table 3: Missing periods in the measured data

	N miss	N day	N after	N 10%	N 5 %
1	4	3	14	4	9
2	41	63	24	106	404
3	12	15	69	10	30
4	1	1	43	1	2
5	1	1	7	1	2
6	1	1	40	1	2
7	1	1	19	1	2
8	18	31	462	16	89
9	3	3	288	3	7

Table 4 shows the estimated load for each of the missing periods. The estimated loads are much higher in magnitude than the measured loads before and after the missing period, figure 8 shows the load estimated using 5% g-effect cut off, 10% g-effect cut off and from ambient temperature. The high estimated loads implies that the model underestimates the effect of the load on the fluid temperature.

Figure 9 shows the measured fluid temperature and estimated temperatures for the whole period using the estimated loads from the 10% g-effect case for the missing periods measured The simulated fluid temperatures have a good agreement between measured and simulated temperature. The overall mean absolute error (MAE) between the measured and the simulated data is 1.39K for the 10% g-effect cut off case and

Table 4: Estimated loads

Missing period	Qe 10%		Qe 5%	
	QA	QB	QA	QB
1	1238	2160	1657	2766
3	-6856	-702	-7567	-1556
4	-3406	-373	-2516	-398
5	3154	-4315	3681	-3339
6	2603	122	2745	337
7	3315	697	3951	1305
8	6126	3000	6423	3402
9	666	151	484	172

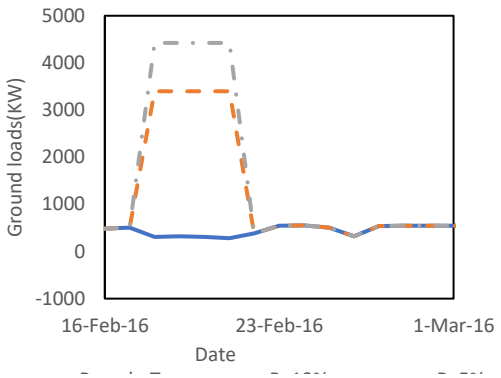

Figure 8: estimated loads for the first missing period

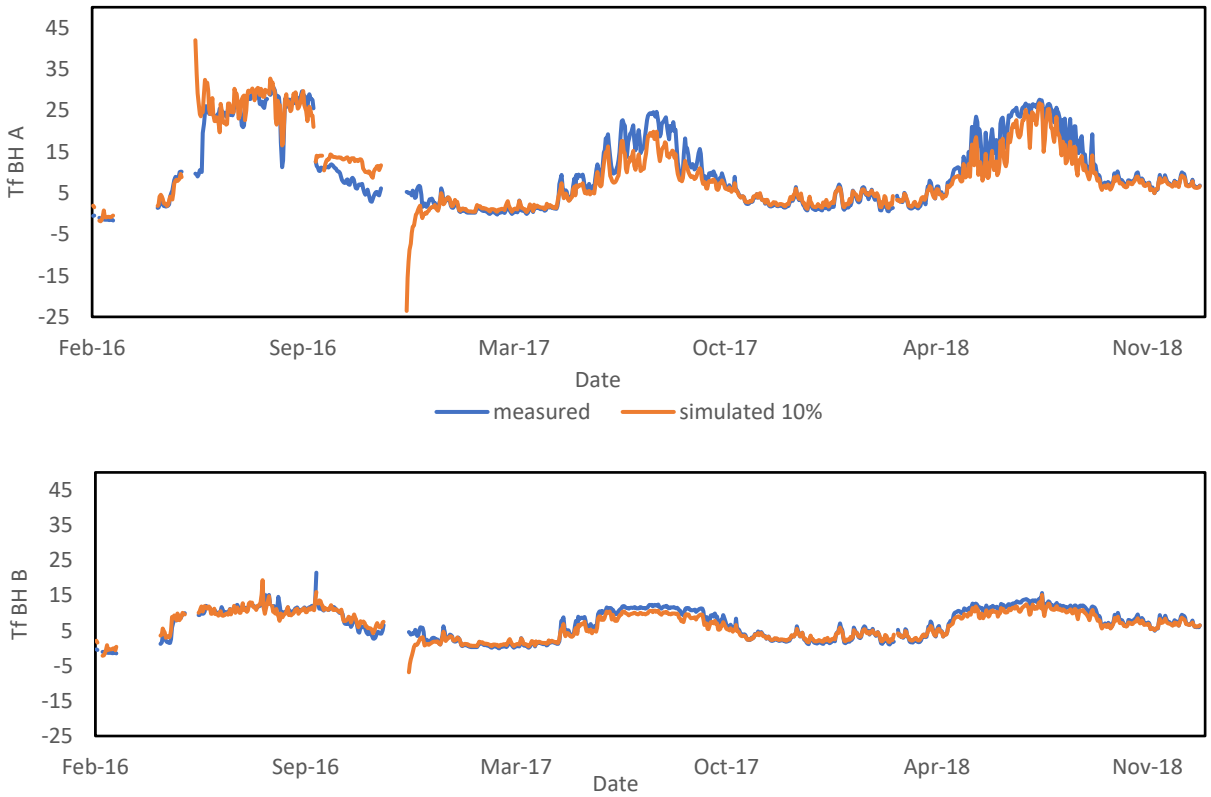

Figure 9: Comparison of measured and simulated fluid temperatures using estimated missing loads

1.46K for the 5% g-effect cut off case, while the MAE for the case where the missing data is estimated using the ambient temperature is 1.54K. Hence, the high loads estimated for missing periods reduces the overall deviation of the model. The adverse effect of the high load is seen immediately after the missing period, before the period used for minimising the minimisation, i.e., the period with aggregated steps. In this period the model with missing load from ambient temperature performs better than the other two cases. The deviation for this period is higher for the 5% g-effect cut off case compared to the 10% g-effect cut off case.

7. CONCLUSIONS

A method to estimate the heat load of the BHE during periods of missing data was proposed. The method estimates the missing data by minimizing the difference between measured and simulated fluid temperatures for a period after the missing data.

The method predicted the missing load with negligible error for an ideal case without model or measurement error. We recommended a time period of fluid temperatures used for minimization. The lower limit of the time period is based on an aggregation scheme that is used to define the time after the missing data when the time resolution of 1 day can be used. The upper limit is set to a period when the effect of the missing load is significant.

The sensitivity of estimating the missing load to error in measured load and fluid temperature was determined. The missing load has a high sensitivity to both the parameters hence to accurately determine the missing load the measured data and the model used for determining the fluid temperatures must have high accuracy. The proposed method was applied to a monitored BHE with missing loads. The predicted missing loads were unreasonably high but the overall deviation between the simulated and measured fluid temperature reduced. This shows that the estimated missing loads corrects the errors of the model.

REFRENCES

*Atam, E. and L. Helsen (2016). "Ground-coupled heat pumps: Part 1–Literature review and research challenges in modeling and optimal control." Renewable Sustainable Energy Reviews **54**: 1653-1667.*

*Bernier, M. A., P. Pinel, R. Labib and R. Paillot (2004). "A multiple load aggregation algorithm for annual hourly simulations of GCHP systems." Hvac&R Research **10**(4): 471-487.*

*Claesson, J. and S. Javed (2012). "A Load-Aggregation Method to Calculate Extraction Temperatures of Borehole Heat Exchangers." Ashrae Transactions 2012, Vol 118, Pt 1 **118**(1): 530-539.*

*Cullin, J. R., J. D. Spitler, C. Montagud, F. Ruiz-Calvo, S. J. Rees, S. S. Naicker, P. Konecny and L. E. Southard (2015). "Validation of vertical ground heat exchanger design methodologies." Science and Technology for the Built Environment **21**(2): 137-149.*

*De Rosa, M., F. Ruiz-Calvo, J. M. Corberán, C. Montagud and L. A. Tagliafico (2015). "A novel TRNSYS type for short-term borehole heat exchanger simulation: B2G model." Energy conversion management **100**: 347-357.*

*Esen, H., M. Inalli, A. Sengur and M. Esen (2008). "Modeling a ground-coupled heat pump system by a support vector machine." Renewable Energy **33**(8): 1814-1823.*

*Esen, H., M. Inalli, A. Sengur and M. Esen (2008). "Modelling a ground-coupled heat pump system using adaptive neuro-fuzzy inference systems." International Journal of Refrigeration-Revue Internationale Du Froid **31**(1): 65-74.*

*Esen, H., M. Inalli, A. Sengur and M. Esen (2008). "Performance prediction of a ground-coupled heat pump system using artificial neural networks." Expert Systems with Applications **35**(4): 1940-1948.*

*Fernandez, M., P. Eguia, E. Granada and L. Febrero (2017). "Sensitivity analysis of a vertical geothermal heat exchanger dynamic simulation: Calibration and error determination." Geothermics **70**: 249-259.*

*Hellström, G., B. Sanner, M. Klugescheid, T. Gonka and S. Mårtensson (1997). Experiences with the borehole heat exchanger software EED. Proc. Megastock. Sapporo, Japan. **97:** 247-252.*

*Kim, S.-K., G.-O. Bae, K.-K. Lee and Y. Song (2010). "Field-scale evaluation of the design of borehole heat exchangers for the use of shallow geothermal energy." Energy **35**(2): 491-500.*

*Lamarche, L. (2009). "A fast algorithm for the hourly simulations of ground-source heat pumps using arbitrary response factors." Renewable Energy **34**(10): 2252-2258.*

*Lamarche, L. (2017). "Mixed arrangement of multiple input-output borehole systems." Applied Thermal Engineering **124**: 466-476.*

*Li, M. and A. C. K. Lai (2015). "Review of analytical models for heat transfer by vertical ground heat exchangers (GHEs): A perspective of time and space scales." Applied Energy **151**: 178-191.*

*McDaniel, A., D. Fratta, J. M. Tinjum and D. J. Hart (2018). "Long-term district-scale geothermal exchange borefield monitoring with fiber optic distributed temperature sensing." Geothermics **72**: 193-204.*

*Michopoulos, A., D. Bozis, P. Kikidis, K. Papakostas and N. A. Kyriakis (2007). "Three-years operation experience of a ground source heat pump system in Northern Greece." Energy and Buildings **39**(3): 328-334.*

*Michopoulos, A., T. Zachariadis and N. Kyriakis (2013). "Operation characteristics and experience of a ground source heat pump system with a vertical ground heat exchanger." Energy **51**: 349-357.*

*Monzo, P., A. R. Puttige, J. Acuna, P. Mogensen, A. Cazorla, J. Rodriguez, C. Montagud and F. Cerdeira (2018). "Numerical modeling of ground thermal response with borehole heat exchangers connected in parallel." Energy and Buildings **172**: 371-384.*

Naiker, S. and S. Rees (2011). Monitoring and performance analysis of a large non-domestic ground source heat pump installation. CIBSE Technical Symposium,, Leicester, UK, CIBSE.

*Ruiz-Calvo, F., J. Cervera-Vazquez, C. Montagud and J. M. Corberan (2016). "Reference data sets for validating and analyzing GSHP systems based on an eleven-year operation period." Geothermics **64**: 538-550.*

*Ruiz-Calvo, F. and C. Montagud (2014). "Reference data sets for validating GSHP system models and analyzing performance parameters based on a five-year operation period." Geothermics **51**: 417-428.*

Sanner, B. (2017). Ground Source Heat Pumps–history, development, current status, and future prospects. Proceedings of 12th IEA Heat Pump Conference (paper K. 2.9.). , Rotterdam.

*Tordrup, K. W., S. E. Poulsen and H. Bjorn (2017). "An improved method for upscaling borehole thermal energy storage using inverse finite element modelling." Renewable Energy **105**: 13-21.*

*Yang, H., P. Cui and Z. Fang (2010). "Vertical-borehole ground-coupled heat pumps: A review of models and systems." Applied Energy **87**(1): 16-27.*

*Yavuzturk, C. and J. D. Spitler (1999). "A short time step response factor model for vertical ground loop heat exchangers." Ashrae Transactions **105**(2): 475-485.*

*Zeng, H., N. Diao and Z. Fang (2002). "A finite line-source model for boreholes in geothermal heat exchangers." Heat Transfer—Asian Research: Co-sponsored by the Society of Chemical Engineers of Japan the Heat Transfer Division of ASME **31**(7): 558-567.*